0D Modeling of Ion Cyclotron Wall Conditioning plasmas

T. Wauters[1], D. Douai[1], A. Lyssoivan[2], V. Philipps[3], O. Marchuk[3], D. Wünderlich[4], S. Brémond[1], M. Freisinger[3], A. Kreter[3], G. Lombard[1], P. Mollard[1], B. Pegourié[1], H. Reimer[3], G. Sergienko[3], M. Vervier[2], G. Van Wassenhove[2], M. Van Schoor[2], and G. Van Oost[5]

[1] *CEA, IRFM, Association Euratom-CEA, 13108 St Paul lez Durance, France*

[2] *LPP-ERM/KMS, Association Euratom-Belgian State, 1000 Brussels, Belgium*

[3] *IEF-Plasmaphysik FZ Jülich, Euratom Association, 52425 Jülich, Germany*

[4] *Max-Planck Institut für Plasmaphysik, Euratom Association, 85748 Garching, Germany*

[5] *Ghent University, Department of Applied Physics, 9000 Ghent, Belgium*

Introduction

Results of the recently developed 0D kinetic model for hydrogen-helium RF discharges in toroidal magnetic configurations, TOMATOR-0D, are presented. The modeling efforts are mainly motivated by the urgent need to consolidate the Ion Cyclotron Wall Conditioning (ICWC) technique, which is the main envisaged technique for the conditioning of the ITER first wall in the presence of the toroidal magnetic field [1]. The model has been developed to obtain insight on ICRF plasma parameters, particle fluxes to the walls and the main collisional processes, the latter being the fundamental mechanism for the build-up of a plasma. This is of particular importance since most standard tokamak plasma diagnostics are not adapted to accurately diagnose the typical low temperature and low density RF plasmas. To describe numerically in a 0D approach the evolution of ICRF plasma parameters in tokamaks and stellarators, a set of transport equations [2, 3, 4] was adopted. In the present model these equations are updated to include molecular hydrogen and helium, which is especially of importance for wall conditioning plasmas. The model reproduces experimental plasma density dependencies on discharge pressure and coupled RF power, both for hydrogen RF discharges ($n_e \approx 1-5\cdot 10^{10}\,\mathrm{cm}^{-3}$) as for helium discharges ($n_e \approx 1-5\cdot 10^{11}\,\mathrm{cm}^{-3}$), found on TEXTOR and Tore Supra.

Balance equations

The 0D plasma description is based on energy and particle balance equations for 9 principal species: H, H^+, H_2, H_2^+, H_3^+, He, He^+, He^{2+} and e^-. It takes into account (1) elementary atomic and molecular collision processes, such as excitation/radiation, ionization, dissociation, recombination, charge exchange, etc... (2) elastic collisions, (3) particle losses due to the finite plasma volume and confinement properties of the magnetic configuration, and particle recycling (4) active pumping and gas injection, (5) RF heating of electrons (and protons) and (6) a qualitative description of plasma impurities (carbon). The model does not treat excited states as

separate species. Since cross sections are mostly dependent on the excited state of the involved particle, radiative-collisional models (RC) [5, 6] are applied where possible to obtain effective rate coefficients.

H_2-ICWC simulation

Fig. 1 shows modeling results (red lines) for a Tore Supra H_2-ICWC discharge with $P_{\mathrm{RF,gen}} = 75\,\mathrm{kW}$ and $p_{H_2} = 1.3 \cdot 10^{-4}\,\mathrm{mbar}$. The employed model inputs are the neutral gas injection rate (constant during the whole discharge), the impurity content (0.8% of the neutral pressure before breakdown), the vessel volume and pumping speed, the wall recycling coefficient R and the maximum coupled RF power. The hydrogen pressure (baratron), coupled RF power and plasma density (averaged over 5 central vertical DCN interferometry lines, $\sim 1\,\mathrm{m}$) are plotted separately. Two main phases can be distinguished from the figure. During the breakdown phase ($0 - 1.2\,\mathrm{s}$), the neutral pressure remains unchanged and the plasma density is out of measurement reach although the RF antenna is powered, until a sudden increase of the plasma density and RF coupling efficiency is noticeable together with a drop in pressure. Electron collisional processes, well described in the model, are the fundamental mechanism for the build-up of the ICRF plasma. The plasma breakdown moment is generally indicated by a sudden drop in antenna voltage (not shown on the figure). During the plasma phase ($> 1.2\,\mathrm{s}$) the density remains practically unchanged around $n_e = 1.3 \cdot 10^{17}\,\mathrm{m}^{-3}$. The electron, hydrogen atom and hydrogen ion temperatures during the steady state phase equal $T_e = 3.5\,\mathrm{eV}$, $T_{\mathrm{H}} = 3.7\,\mathrm{eV}$ and $T_{\mathrm{H}^+} = 3.0\,\mathrm{eV}$, respectively.

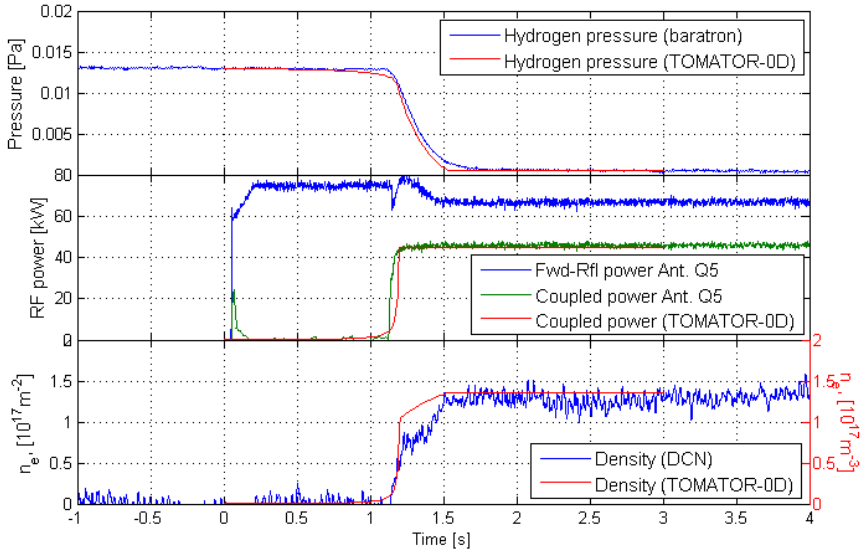

Figure 1: Tore Supra H_2-ICWC discharge (TS45699, third RF pulse, $P_{\mathrm{RF,gen}} = 75\,\mathrm{kW}$, $p_{H_2} = 1.3 \cdot 10^{-4}\,\mathrm{mbar}$). Top to bottom: exp. and modeled (red lines) hydrogen pressure, coupl. RF power and plasma density.

The coupled RF-power in the plasma breakdown phase is proportional to the electron density. The nominal RF power is thus only partially coupled when the electron density is low compared to the neutral density. To simulate plasma breakdown with the 0D model the α-scaling, previ-

ously adopted by Moiseensko [3] and successfully used in the 0D model version for atomic hydrogen [7], was expanded for hydrogen-helium plasmas:

$$P_{\mathrm{RF,coup}} = \begin{cases} P_{\mathrm{RF,max}} f_\alpha / \alpha & \text{if } f_\alpha < \alpha \\ P_{\mathrm{RF,max}} & \text{if } f_\alpha \geq \alpha \end{cases}, \text{ where } f_\alpha = \frac{n_e}{n_e + n_\mathrm{H} + n_{\mathrm{H}_2} + n_\mathrm{He}}. \quad (1)$$

Above a degree of ionization represented by α the maximum RF power will be coupled. The hydrogen RF plasma (Fig. 1) was simulated using $\alpha = 0.044$. The sudden increase of coupled power during plasma breakdown obtained from the antenna resistance is reproduced by the 0D model. The simultaneous pressure drop is mainly due to the consumption of particles by the walls. Upon discharge initiation a transient storage of particles is observed, governed by a low recycling coefficient of $R = 0.92$. An equilibrium between the particle flux to the wall and the wall release rate is reached rapidly, resulting in a much higher recycling coefficient during the plasma phase $R = 0.984$, which is about 1% lower as found in [8].

Wall fluxes, particle recycling and retention

Fig. 2 summarizes the particle fluxes to the walls (mainly H and H^+, resp. blue and green lines), the injection rate of hydrogen molecules (normalized to wall surface and number of atoms, red line), the removal rate of hydrogen molecules by the pumps (cyan line), and the retention rate of hydrogen into the wall (purple line). Before plasma breakdown, the hydrogen evacuation rate by the machine pumps equals the gas injection rate, leading to a stable vessel pressure of $p_{\mathrm{H}_2} = 1.3 \cdot 10^{-4}$ mbar. At the plasma breakdown moment ($t \approx 1.2$ s) the atomic hydrogen wall flux peaks to a value of the order of $\Phi_\mathrm{H} \approx 10^{20}\,/\mathrm{sm}^2$, where after due to the decreasing pressure the atom flux decreases to $\sim 1.8 \cdot 10^{19}\,/\mathrm{sm}^2$. These modeled values are in agreement with estimated total wall fluxes from particle balance analysis [8]. The ion wall flux is much lower, and behaves proportional to the electron density. The steady state value during the plasma phase is of the order of $\Phi_{\mathrm{H}^+} \approx 6.0 \cdot 10^{17}\,/\mathrm{sm}^2$, in agreement with ion currents collected on the ALT limiter blades in TEXTOR during hydrogen ICWC discharges. The retention at the start of the discharge accounts for a total of $\sim 5 \cdot 10^{19}$ particles. It is

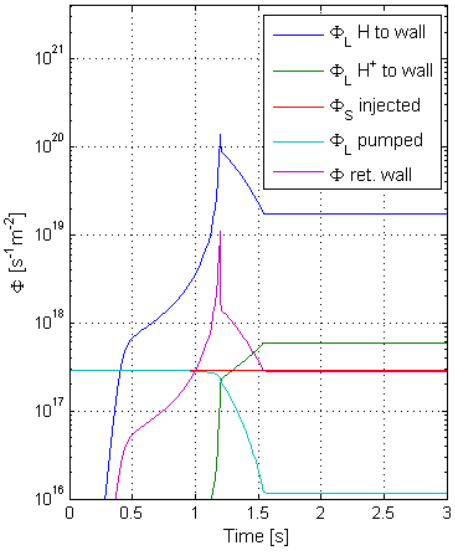

Figure 2: Modeled particle wall flux, injection rate by valves and retention rate.

expected that a large part of these particles are transiently stored and are retrieved from the wall after the RF pulse, which causes the typical out-gassing peak as described in [9]. The retention rate during the steady state plasma phase ($t > 1.5\,\mathrm{s}$) equals the injection rate minus the removal rate by the pumps, and is approximately equal to the injection rate of particles into the vessel ($\sim 2.9 \cdot 10^{17}\,/\mathrm{sm}^2$) due to the low pressure during this phase ($p_{H_2} \approx 5 \cdot 10^{-6}\,\mathrm{mbar}$). It is expected from the stable density and pressure time traces (Fig. 1) that these particles are permanently stored in the vessel, which corresponds for this $\approx 4\,\mathrm{s}$ RF discharge to a permanent retention of $\sim 8 \cdot 10^{19}$ particles, which is of the same order as found in [8]. ICWC isotope exchange experiments on both TEXTOR and Tore Supra revealed indeed that the total amount of permanently retained particles increases on increasing RF pulse length.

Conclusion

The presented 0D ICWC plasma model allows to reproduce experimental pressure, density and coupled power time traces of a Tore Supra H_2-ICWC discharge from discharge initiation to steady state plasma, and gives insight into the particle wall fluxes and retention rates. The wall interaction, represented in the model by a particle recycling coefficient, has a major influence on the neutral pressure (constant injection) and plasma density in H_2-ICWC discharges. During the breakdown phase particles are transiently stored in the wall causing a steep pressure drop while during the plasma phase an equilibrium pressure is formed where the gas injection rate approximately equals the permanent hydrogen retention rate. Employing shorter RF pulses ($1 \sim 2\,\mathrm{s}$) is favored to limit retention, while maximizing the recovery of transiently stored particles [8, 9].

Acknowledgments

This work was supported by EURATOM and carried out within the framework of the European Fusion Development Agreement. The views and opinions expressed herein do not necessarily reflect those of the European Commission.

References

[1] M. Shimada and R. A. Pitts, J. Nucl. Mat. *doi:10.1016/j.jnucmat.2010.11.085*, (2010).
[2] A. Lyssoivan and et al., Nucl. Fusion **32**, 1361 (1992).
[3] V. E. Moiseenko and et al., Fusion Eng. & Design **26**, 203 (1995).
[4] B. Lloyd, P. G. Carolan, and C. D. Warrick, Plasma Phys. & Controlled Fusion **38**, 1627 (1996).
[5] D. Wünderlich, S. Dietrich, and U. Fantz, J. Quant. Spectrosc. Radiat. Transfer **110**, 62 (2009).
[6] Y. V. Ralchenko and Y. Maron, J. Quant. Spectrosc. Radiat. Transfer **71**, 609 (2001).
[7] A. Lyssoivan et al., *AIP Confer. Series*, volume 1187, pages 165–172, (2009).
[8] T. Wauters et al., J. Nucl. Mat. *doi:10.1016/j.jnucmat.2010.11.072*, (2010).
[9] D. Douai et al., J. Nucl. Mat. *doi:10.1016/j.jnucmat.2010.11.083*, (2010).